4th International Conference of Engineering Division,
National Research Center, Cairo, Egypt
Steps Towards Innovative Sustainable Development
NRC-ICED 2018
May 6-8, 2018
Cairo, Egypt

Coupled Vibration Analysis of Composite Wind Turbine Blades

Karam Y. Maalawi[1] and Gerges E. Beshay[2]

1) Mechanical Engineering Department, National Research Centre, , Dokki, 12311, Cairo, Egypt; nrc.aero@gmail.com
2) Mechanical Engineering Department, Shoubra Faculty of Engineering, Cairo, Egypt; Gerges.Beshay@feng.bu.edu.eg

Abstract

An analytical model for the free vibration of non-uniform, anisotropic, thin-walled wind turbine blade is presented. The blade is constructed from laminated fibrous composite materials with variable thickness and stiffness. The study focuses on the blade spar that represents the main supporting structure within a wind turbine blade. Two specific lay-up configurations; namely, Circumferentially Asymmetric Stiffness (***CAS***) and Circumferentially Uniform Stiffness (***CUS***) are analyzed. The transfer matrix method is used to study the vibration behavior of a tapered spar by dividing it into multiple uniform segments, each of which has different length, cross sectional dimensions and material properties. The influence of coupling on the vibration modes is identified and the functional behavior of the frequencies with the lamination parameters is thoroughly investigated and discussed.

Key words: Wind energy, Wind turbine, Composite blade, Natural frequencies, Transfer matrix.

1. Introduction

Among all renewable energies of different styles, wind energy is the most popularized and potentially applicable type of green energy. Because larger wind turbines have more power capture and economical advantages, the typical size of utility-scale wind turbines, shown in Fig. 1, has grown dramatically over the last three decades [1, 2]. Such large flexible configuration operating in uncertain environments, gives rise to significant vibration problems, and assesses the importance of analyzing structural dynamics in the design of successful wind turbine systems. This study focuses on wind turbine blade free vibration analysis using a simplified model of uniform anisotropic thin-walled closed-section beams [3]. This model is applied to the blade spar structure with closed cross section made of laminated fibrous composite materials with variable thickness and stiffness. More investigations to study the influence of coupling between the different vibration modes are given by Dancila and Armanios [4].

The main motivation for this research work is to analyze the functional behavior of the blade frequency by tailoring the structural mass and stiffness distributions along the entire span. The study is focused on the spar structure that represents the main load carrying component of the wind turbine blade. Material grading concept is achieved by changing the fiber content throughout the blade structure. Design parameters include the volume fraction distribution of the constituent materials of construction as well as geometric and cross-sectional parameters of the blade. The blade is assumed to have a large span-to-chord ratio, which enabled us to model the main spar as an equivalent straight beam, positioned along the elastic axis. Structural analyses are performed using simplified mathematical expressions by implementing the conventional beam and classical lamination theories. The governing differential equations of motion are derived and solved for the coupled extensional-torsional and flexural-torsional modes of vibration. The transfer matrix method is implemented to obtain the required analytical solutions. Finally, the relevant concluding remarks and recommendations for future studies are given and discussed.

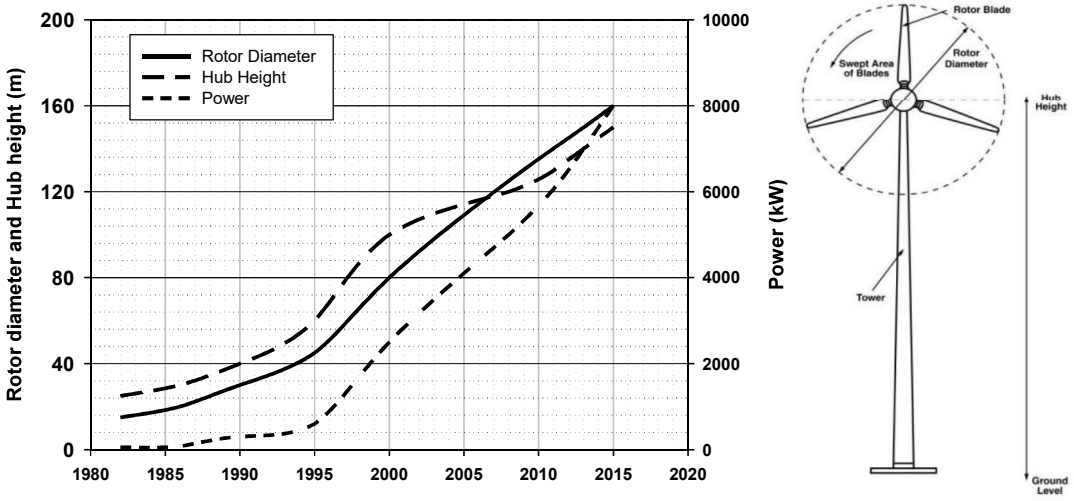

Figure 1. Size and power increase of commercial wind turbines [1]

2. Structural Analysis

Figure 2 shows the structural model of the blade spar, which is represented by a thin-walled cantilever beam consisted of N*s* uniform segments. Each segment has different dimensions and material properties that satisfying the geometrical tapering and material grading concepts. Any segment k with length L_k has a rectangular cross section with dimensions, width b_k , depth a_k and wall thickness H_k. Each segment is a uniform laminated fibrous composite beam consisted of Nr layers each of which has thickness h_j, fiber volume fraction V_{fj}, and fiber orientation angle θ_j. The constitutive relationships in terms of stress resultants and kinematic variables are [3, 4]:

$$\begin{bmatrix} T \\ M_x \\ M_y \\ M_z \end{bmatrix} = \begin{bmatrix} C_{11} & C_{12} & C_{13} & C_{14} \\ C_{12} & C_{22} & C_{23} & C_{24} \\ C_{13} & C_{23} & C_{33} & C_{34} \\ C_{14} & C_{24} & C_{34} & C_{44} \end{bmatrix} \begin{bmatrix} U_1' \\ \varphi' \\ U_3'' \\ U_2'' \end{bmatrix} \tag{1}$$

where T is the tensile force, M_x is the torsional moment, M_y and M_z are bending moments about *y* and *z* axes respectively. C_{mn} are called the beam cross sectional stiffness coefficients and U_1, U_2, and U_3 are the average cross-sectional displacements along *x*, *y*, and *z* coordinates, respectively, and $\varphi(x)$ is the cross-sectional rotation function. The superscript prime means a differentiation with respect to x.

The equations of motion can be obtained using Hamilton's principle. For the case of undamped free vibration, the resulting system of equations is [4]:

$$\begin{aligned} C_{11}U_1'' + C_{12}\varphi'' + C_{13}U_3''' + C_{14}U_2''' - m\ddot{U}_1 &= 0 \\ C_{12}U_1'' + C_{22}\varphi'' + C_{23}U_3''' + C_{24}U_2''' - I\ddot{\varphi} - S_z\ddot{U}_3 + S_y\ddot{U}_2 &= 0 \\ C_{13}U_1''' + C_{23}\varphi''' + C_{33}U_3'''' + C_{34}U_2'''' + S_z\ddot{\varphi} + m\ddot{U}_3 &= 0 \\ C_{14}U_1''' + C_{24}\varphi''' + C_{34}U_3'''' + C_{44}U_2'''' - S_y\ddot{\varphi} + m\ddot{U}_2 &= 0 \end{aligned} \tag{2}$$

Where *m*, I, S_z and S_y are the mass, polar, and first moments of inertia per unit length of the beam, respectively. The prime and dot superscripts denote differentiation with respect to x and time, respectively.

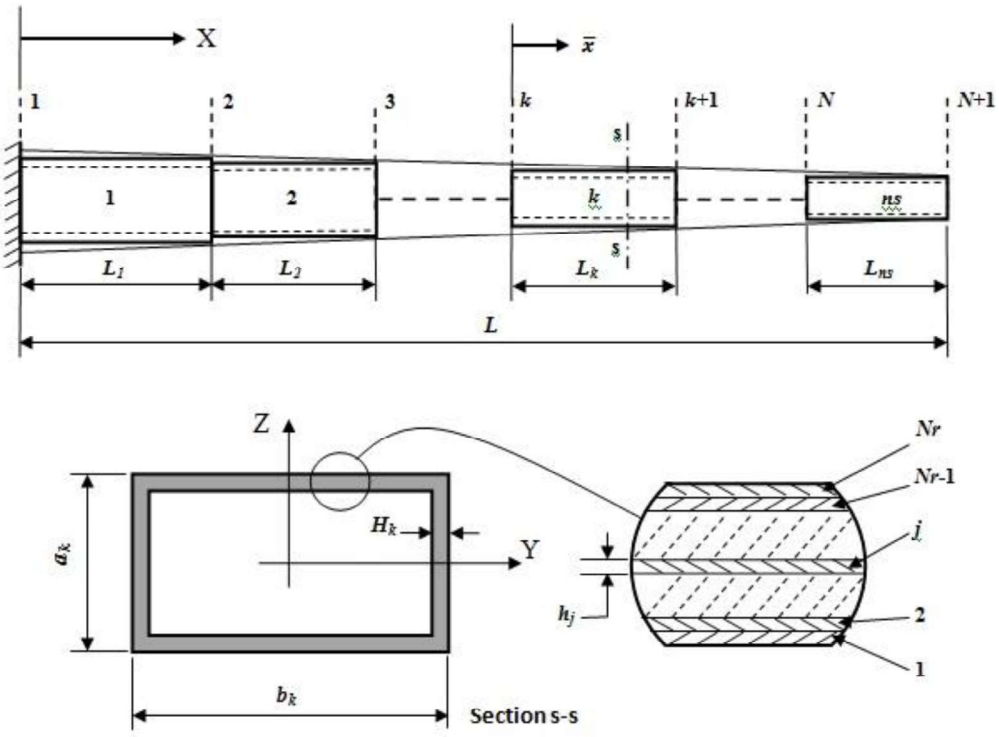

Figure 2 Blade spar structural model

A closed form solution for the most general case of the equations of motion (Eq. 2) is not available. Two particular cases of fiber layup are considered in which some of stiffness coefficients vanish. The first case is called circumferentially uniform stiffness (CUS) and the second circumferentially asymmetric stiffness (CAS). Figure 3 shows a rectangular cross-sectional beam segment with both CUS and CAS layup configurations. CUS layup configuration is manufactured by warping the composite layup using filament winding technique, $\theta(-z) = \theta(z)$, while, CAS layup configuration is manufactured such that the beam cross section is symmetric about *OXY* plane. $\theta(-z) = -\theta(z)$.

2.1 CUS Layup Configuration

For any segment ***k*** within the blade structure, a local coordinate system with $\bar{X}$-axis is introduced such that (see Fig.2):

$$0 \leq \bar{x} = X - X_k \leq L_k \tag{3}$$

In the special case of CUS layup, the equations of motion reduce to (for the k^{th} segment):

$$\begin{aligned} C_{11}^k U_1'' + C_{12}^k \varphi'' - m_k \ddot{U}_1 &= 0 \\ C_{12}^k U_1'' + C_{22}^k \varphi'' - I_k \ddot{\varphi} &= 0 \\ C_{33}^k U_3'''' + m_k \ddot{U}_3 &= 0 \\ C_{44}^k U_2'''' + m_k \ddot{U}_2 &= 0 \end{aligned} \tag{4}$$

The first two equations are expressing a coupled extension-twist vibration (ETV) mode, while the third and fourth equations are expressing vertical bending vibration (VBV) and horizontal bending vibration (HBV) modes respectively.

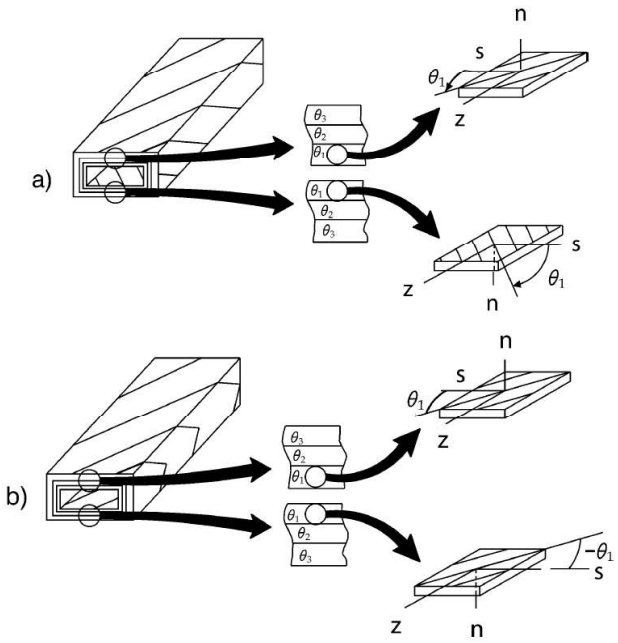

Figure 3 Spar segment with (a) CUS and (b) CAS layup configurations

For rectangular cross section, the stiffness coefficients are given by [5]

$$
\begin{aligned}
C_{11}^k &= 2K_A^k(b_k + a_k - 2H_k) \\
C_{12}^k &= K_B^k(b_k - H_k)(a_k - H_k) \\
C_{22}^k &= K_C^k \frac{\left((b_k - H_k)(a_k - H_k)\right)^2}{2(b_k + a_k - 2H_k)} \\
C_{33}^k &= \left(K_A^k - \frac{{K_B^k}^2}{K_C^k}\right)\left(\frac{(a_k - H_k)^3}{6}\right)\left(1 + \frac{3(b_k - H_k)}{(a_k - H_k)}\right) \\
C_{44}^k &= \left(K_A^k - \frac{{K_B^k}^2}{K_C^k}\right)\left(\frac{(b_k - H_k)^3}{6}\right)\left(1 + \frac{3(a_k - H_k)}{(b_k - H_k)}\right)
\end{aligned}
\tag{5}
$$

where K_A, K_B, and K_C are the reduced axial, coupled axial-shear, and shear stiffness coefficients, respectively of a laminated composite beam:

$$
\begin{aligned}
K_A &= A_{11} - \frac{(A_{12})^2}{A_{22}} \\
K_B &= 2\left[A_{16} - \frac{A_{12}A_{26}}{A_{22}}\right] \\
K_C &= 4\left[A_{66} - \frac{(A_{26})^2}{A_{22}}\right]
\end{aligned}
\tag{6}
$$

A_{mn} are the membrane extensional stiffness coefficients of a laminate that can be calculated from general stiffness matrix of the classical laminate theory [6]. Considering the equations of coupled extension-twist vibration, the assumed solution is:

$$
\begin{aligned}
U_1(x,t) &= \bar{C}_1 e^{\lambda x + i\omega t} \\
\varphi(x,t) &= \bar{C}_2 e^{\lambda x + i\omega t}
\end{aligned}
\tag{7}
$$

where, ω is the natural circular frequency of free vibration. Substituting from (7) into (4), the associated characteristic equation can be shown to be:

$$\left(C_{11}^k C_{22}^k - C_{12}^{k\,2}\right)\lambda^4 + (C_{11}^k I_k + C_{22}^k m_k)\omega^2\lambda^2 + m_k I_k \omega^4 = 0 \tag{8a}$$

That can be expressed as:

$$a\lambda^4 + b\omega^2\lambda^2 + c\omega^4 = 0$$

where

$$\begin{aligned} a &= C_{11}^k C_{22}^k - C_{12}^{k\,2} \\ b &= C_{11}^k I_k + C_{22}^k m_k \\ c &= m_k I_k \end{aligned} \tag{8b}$$

The solution of the characteristic equation can be expressed as:

$$\begin{aligned} \lambda_{1,2} &= \pm i\omega \sqrt{\frac{b - \sqrt{b^2 - 4ac}}{2a}} = \pm i\alpha_1 \\ \lambda_{3,4} &= \pm i\omega \sqrt{\frac{b + \sqrt{b^2 - 4ac}}{2a}} = \pm i\alpha_2 \end{aligned} \tag{8c}$$

where

$$\alpha_{1,2} = \omega \sqrt{\frac{b \mp \sqrt{b^2 - 4ac}}{2a}} \tag{8d}$$

If $C_{11}^k I_k > C_{22}^k m_k$, then the minus sign in Eq. (8c) will generate natural frequencies with axial-mode dominated vibration, while the plus sign will generate natural frequencies with torsion-mode dominated vibration. If $C_{11}^k I_k < C_{22}^k m_k$, the domination is reversed. The general solution of the coupled extension-twist vibration problem (Eq. 4) can be expressed as:

$$\begin{aligned} U_1(x,t) &= (c_1 \sin\alpha_1 x + c_2 \cos\alpha_1 x + c_3 \sin\alpha_2 x + c_4 \cos\alpha_2 x)e^{i\omega t} \\ \varphi(x,t) &= (c_5 \sin\alpha_1 x + c_6 \cos\alpha_1 x + c_7 \sin\alpha_2 x + c_8 \cos\alpha_2 x)e^{i\omega t} \end{aligned} \tag{9}$$

In order to satisfy both the coupled equations of motion, there are specific relations between the constants such that:

$$\begin{aligned} c_5 = q_1 c_1, \quad c_6 = q_1 c_2, \quad c_7 = q_2 c_3, \quad c_8 = q_2 c_4 \\ q_{1,2} = \frac{2m_k a}{C_{12}^k\left(b \mp \sqrt{b^2 - 4ac}\right)} - \frac{C_{11}^k}{C_{12}^k} \end{aligned} \tag{10}$$

2.2 CAS Layup Configuration

In this case, the equations of motion, applied to segment ***k***, are reduced to:

$$\begin{aligned} C_{11}^k U_1'' - m_k \ddot{U}_1 &= 0 \\ C_{22}^k \varphi'' + C_{23}^k U_3''' - I_k \ddot{\varphi} &= 0 \\ C_{23}^k \varphi''' + C_{33}^k U_3'''' + m_k \ddot{U}_3 &= 0 \\ C_{44}^k U_2'''' + m_k \ddot{U}_2 &= 0 \end{aligned} \tag{11}$$

The second and third equations of motion are expressing a coupled bending-twist vibration (BTV) mode, while the first and fourth equations of motion are expressing extension vibration (EV) and horizontal bending vibration (HBV) modes, respectively. The non-zero stiffness coefficients are given by:

$$\begin{aligned} C_{11}^k &= 2K_A^k(b_k + a_k - 2H_k) - 2\frac{K_B^{k\,2}}{K_C^k}(b_k - H_k) \\ C_{22}^k &= K_C^k \frac{\left((b_k - H_k)(a_k - H_k)\right)^2}{2(b_k - H_k) + (a_k - H_k)} \end{aligned} \tag{12}$$

$$C_{23}^k = K_B^k \frac{\left((b_k - H_k)(a_k - H_k)\right)^2}{2(b_k - H_k) + (a_k - H_k)}$$

$$C_{33}^k = K_A^k \frac{(a_k - H_k)^3}{6}\left[1 + \frac{3(b_k - H_k)}{(a_k - H_k)}\right] - \frac{K_B^{k\,2}}{2K_C^k}\left[1 - \frac{(b_k - H_k)}{(b_k - H_k) + (a_k - H_k)/2}\right](b_k - H_k)(a_k - H_k)^2$$

$$C_{44}^k = \frac{(b_k - H_k)^3}{6}\left[\left(1 + \frac{3(a_k - H_k)}{(b_k - H_k)}\right)K_A^k - \frac{K_B^{k\,2}}{K_C^k}\right]$$

Assuming harmonic solution similar to that given in (7), the characteristic equation is obtained by differentiating (11) to get:

$$\left(C_{22}^k C_{33}^k - C_{23}^{k\,2}\right)\lambda^6 + C_{33}^k I_k \omega^2 \lambda^4 - C_{22}^k m_k \omega^2 \lambda^2 - m_k I_k \omega^4 = 0 \qquad (13)$$

which can be expressed as:

$$a\lambda^6 + b\omega^2\lambda^4 - c\omega^2\lambda^2 - d\omega^4 = 0$$

where

$$\begin{aligned} a &= C_{22}^k C_{33}^k - C_{23}^{k\,2} \\ b &= C_{33}^k I_k \\ c &= C_{22}^k m_k \\ d &= m_k I_k \end{aligned} \qquad (14)$$

The solution of the characteristic equation is:

$$\lambda_{1,2} = \pm i\gamma_1\,, \quad \lambda_{3,4} = \pm i\gamma_2\,, \quad \lambda_{5,6} = \pm\gamma_3 \qquad (15)$$

The general solution takes the form:

$$\begin{aligned} U_2(x,t) &= (c_1 \sin\gamma_1 x + c_2 \cos\gamma_1 x + c_3 \sin\gamma_2 x + c_4 \cos\gamma_2 x + c_5 \sinh\gamma_3 x + c_6 \cosh\gamma_3 x)\, e^{i\omega t} \\ \varphi(x,t) &= (c_7 \sin\gamma_1 x + c_8 \cos\gamma_1 x + c_9 \sin\gamma_2 x + c_{10} \cos\gamma_2 x + c_{11} \sinh\gamma_3 x + c_{12} \cosh\gamma_3 x)\, e^{i\omega t} \end{aligned} \qquad (16)$$

The relations between the constants are given by:

$$\begin{aligned} c_7 &= k_1 c_2\,, \quad & c_9 &= k_2 c_4\,, \quad & c_{11} &= k_3 c_6 \\ c_8 &= -k_1 c_1\,, \quad & c_{10} &= -k_2 c_3\,, \quad & c_{12} &= k_3 c_5 \end{aligned}$$

$$\begin{aligned} k_1 &= \frac{C_{23}^k \gamma_1^3}{C_{22}^k \gamma_1^2 - I_k \omega^2} \\ k_2 &= \frac{C_{23}^k \gamma_2^3}{C_{22}^k \gamma_2^2 - I_k \omega^2} \\ k_3 &= \frac{-C_{23}^k \gamma_3^3}{C_{22}^k \gamma_3^2 + I_k \omega^2} \end{aligned} \qquad (17)$$

3. Analysis by Transfer Matrix Method [7]

The relation between the state vector at one end of a segment $\{Z\}_k$ and that at the other end $\{Z\}_{k+1}$ is given by:

$$\{Z\}_{k+1} = [T]_k \{Z\}_k \qquad (18)$$

where $[T]_k$ is called the elementary transfer matrix. For a spar built up of *Ns* uniform segments, Eq. 18 can be applied at successive stations to obtain:

$$\begin{aligned} \{Z\}_{N+1} &= [T]_o \{Z\}_1 \\ [T]_o &= [T]_N [T]_{N-1} \dots\dots\dots [T]_k \dots\dots\dots [T]_2 [T]_1 \end{aligned} \qquad (19)$$

where the matrix $[T]_o$ is known as the overall transfer matrix, which relates the state vectors at the spar fixed end to the free end at which the boundary conditions are well known. Therefore, applying the boundary conditions at both ends and considering only the nontrivial solutions, the frequency equations can be readily obtained. Derivations of the elementary transfer matrices for different vibration modes are discussed in the following section.

Considering the CUS configuration and defining the elements of the state vector at both ends of the k^{th} segment, the elementary transfer matrix for the coupled extension-twist vibration mode can be expressed as:

$$\begin{bmatrix} U_1(L_k) \\ \varphi(L_k) \\ C_{11}U_1'(L_k) + C_{12}\varphi'(L_k) \\ C_{22}\varphi'(L_k) + C_{12}U_1'(L_k) \end{bmatrix} = \begin{bmatrix} T_{11} & T_{12} & T_{13} & T_{14} \\ T_{21} & T_{22} & T_{23} & T_{24} \\ T_{31} & T_{32} & T_{33} & T_{34} \\ T_{41} & T_{42} & T_{43} & T_{44} \end{bmatrix}_k \begin{bmatrix} U_1(0) \\ \varphi(0) \\ C_{11}U_1'(0) + C_{12}\varphi'(0) \\ C_{22}\varphi'(0) + C_{12}U_1'(0) \end{bmatrix} \tag{20}$$

Imposing the cantilevered boundary conditions on the overall transfer matrix, the overall frequency equation for ***coupled extension-twist vibration*** of the blade spar is given by:

$$T_{33}^o T_{44}^o - T_{34}^o T_{43}^o = 0 \tag{21}$$

For the CAS layup configuration, the transfer matrix for the segment *k* is:

$$\begin{bmatrix} -U_3(L_k) \\ \varphi(L_k) \\ U_3'(L_k) \\ C_{22}^k\varphi'(L_k) + C_{23}^k U_3''(L_k) \\ C_{23}^k\varphi'(L_k) + C_{33}^k U_3''(L_k) \\ C_{33}^k U_3'''(L_k) \end{bmatrix} = \begin{bmatrix} T_{11} & T_{12} & T_{13} & T_{14} & T_{15} & T_{16} \\ T_{21} & T_{22} & T_{23} & T_{24} & T_{25} & T_{26} \\ T_{31} & T_{32} & T_{33} & T_{34} & T_{35} & T_{36} \\ T_{41} & T_{42} & T_{43} & T_{44} & T_{45} & T_{46} \\ T_{51} & T_{52} & T_{53} & T_{54} & T_{55} & T_{56} \\ T_{61} & T_{62} & T_{63} & T_{64} & T_{65} & T_{66} \end{bmatrix}_k \begin{bmatrix} -U_3(0) \\ \varphi(0) \\ U_3'(0) \\ C_{22}^k\varphi'(0) + C_{23}^k U_3''(0) \\ C_{23}^k\varphi'(0) + C_{33}^k U_3''(0) \\ C_{33}^k U_3'''(0) \end{bmatrix} \tag{22}$$

Imposing the cantilevered boundary conditions on the overall transfer matrix, the frequency determinant is given by:
:

$$\begin{vmatrix} T_{44} & T_{45} & T_{46} \\ T_{54} & T_{55} & T_{56} \\ T_{64} & T_{65} & T_{66} \end{vmatrix}_o = 0 \tag{23}$$

The natural frequencies for coupled bending-twist vibration can be obtained numerically by solving the characteristic determinant (23) for γ.

4. Functional Behavior of the Coupled Frequencies

Analysis has been carried out for calculating the natural frequencies and studying their behavior for a specific thin-walled composite spar with CUS layup. The effects of fiber orientation angle, fiber volume fraction, and ply thickness are investigated. Results are presented in a two-dimensional design space such that only two design variables are allowed to change while the others are assigned to specific values. As a case study, the main spar of a medium scale composite blade of a 750-kW horizontal axis wind turbine is analyzed. Full description and technical data can be found in [8]. The blades cross-section having NACA 63-218 airfoil are made of E-glass/epoxy composites with properties given in Table (1). The mass distribution along the blade length is shown in Fig 4.

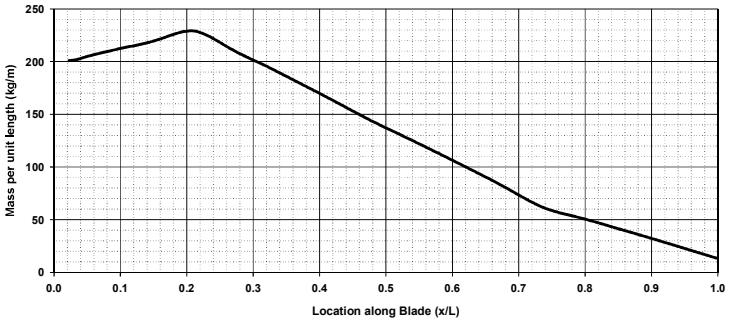

Figure 4 Mass distribution along the blade axis

The spar cross sectional dimensions at root are 340 mm height and 680 mm width, and that at tip 100 mm and 200mm. The chordwise location of the spar cross-section center coincides with the blade pitch axis.

Table 1 Material properties [9]

Property		Epoxy matrix	E-glass fibers
Modulus of elasticity	(GPa)	$E_m = 4.5$	$E_{11f} = E_{22f} = 74$
Modulus of rigidity	(GPa)	$G_m = 1.6$	$G_{12f} = 30$
Poisson's ratio		$\nu_m = 0.4$	$\nu_{12f} = 0.25$
Density	(kg/m^3)	$\rho_m = 1200$	$\rho_f = 2600$
Tensile strength	(MPa)	$\sigma_{mr} = 90$	$\sigma_{11r} = \sigma_{22r} = 3400$
Shear strength	(MPa)	$\tau_{mr} = 52$	------

4.1 Definition of Reference Design

The reference design, to which all the design variables and frequencies are normalized, is selected to be a uniform, thin-walled cantilevered spar made of single unidirectional E-glass/epoxy composite layer (θ_o=0) and fiber volume fraction of V_{fo}=50%. This fiber layup configuration gives maximum natural frequencies for bending and extension modes of vibration while maintain moderate structural mass (m_o=292.5 Kg) and strength. The dimensions of the reference spar are selected according to the mean cross-section dimensions of the wind turbine blade spar under study (see Table 2).

.

Table 2 Dimensions and natural frequencies of the reference design

Dimensions (mm)		Natural frequencies (Hz)			
		Mode	1st	2nd	3rd
Width	b_o= 440				
Height	a_o= 220	Twist	17.59	52.76	87.93
Length	L_o= 18330	Extension	61.99	185.97	309.95
Thickness	H_o=10	Bending	0.65	4.07	11.39

4.2 Case of Single-Segment Spar

Considering a single-segment spar having its walls built up of two composite layers, Fig 5 shows the change in the normalized fundamental frequency of bending or extension in the domain (θ_1, θ_2) with $(V_{fj} = \hat{h}_j = 0.5)$. It is noticed that the maximum natural bending or extension frequency occurs at $(\theta_1, \theta_2) = (0, 0)$ which corresponds to the reference design configuration. The normalized twist-dominated frequency with its maximum occurs near the design point $(\theta_1, \theta_2) = (47, 47)$ is depicted in Fig. 6.

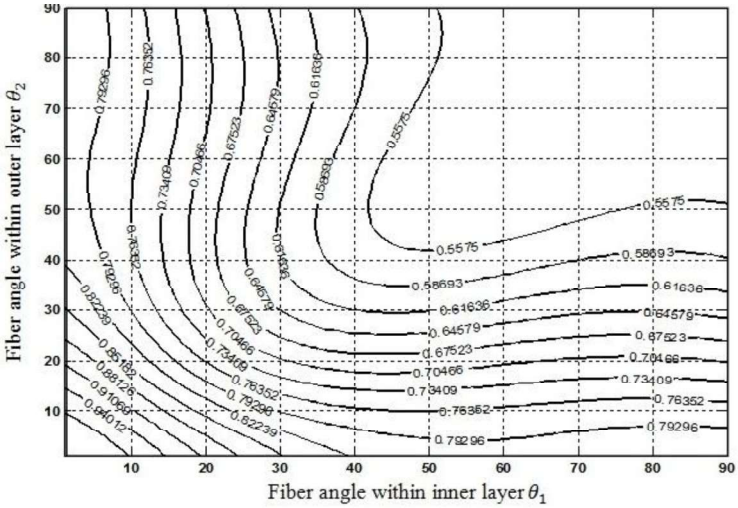

Figure 5 Effect of fiber angles on the normalized bending or extension frequency
(single-segment, two-layer spar, $V_{fj} = \hat{h}_j = 0.5,\ j = 1,2$)

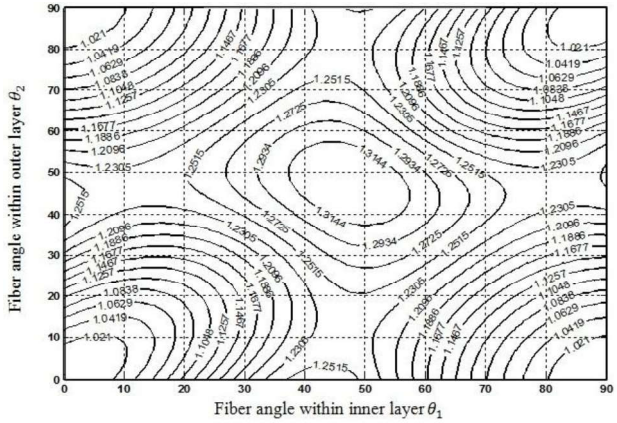

Figure 6 Effect of fiber orientation angles on the normalized twist-dominated frequency
(single-segment, two-layer spar, $V_{fj} = \hat{h}_j = 0.5,\ j = 1,2$)

It is also noticed that the twist-dominated frequency of unidirectional and cross-plies layups, (θ_1, θ_2) = (0, 0), (90, 90), (0, 90), and (90, 0) are the same as that of the reference beam and representing local minima. The layups (θ_1, θ_2) = (0, 45), (45, 0), (45, 90),and (90, 45) give values of twist-dominated natural frequencuy near the maximum value. From the two figures, it is noticed that the frequency level at any combined angles, for example (θ_1, θ_2) = (20, 60), equal to that at (θ_1, θ_2) = (60, 20). Thus the layup stacking sequence doesn't affect the frequency levels. More results for the case $(\theta_j = 0, \hat{h}_j = 0.5)$ have shown that as the volume fraction within the two layers increases, the bending and extension frequencies increase. The maximum twist-dominated frequency can be achieved using material grading concept such that (V_{f1}, V_{f2}) = (min, max). Mass of the beam is directly and linearly proportional to the volume fraction within the two layers of the beam. Also it was found that the stacking sequence doesn't affect the frequency or mass level curves. Considering next the effect of changing thickness of the two layers ($\hat{h}_1$, $\hat{h}_2$) with ($\theta_j = 0, V_{fj} = 0.5$), it was shown that as the thickness of the two layers decrease, the bending and twist-dominated natural frequencies increase. This is due to the decrease in structural mass is more effective than the decrease in stiffness. Change in wall thickness has no effect on frequencies of extension-dominated modes of vibrations. As the wall thickness increases the structural mass increases linearly.

4.3 Case of two-Segment Spar

For a two-segment spar with one layer; the main variables are: $(V_f, \theta j, hj, Lj)_{j=1,2}$. Figure 7 shows the functional behavior of the fundamental bending or twist-dominated frequency in the ($\hat{H}_1$, $\hat{H}_2$)-design space. The maximum natural frequencies occur when wall thickness of the inboard segment is three to four times the reference beam and that of the outboard segment is minimum.

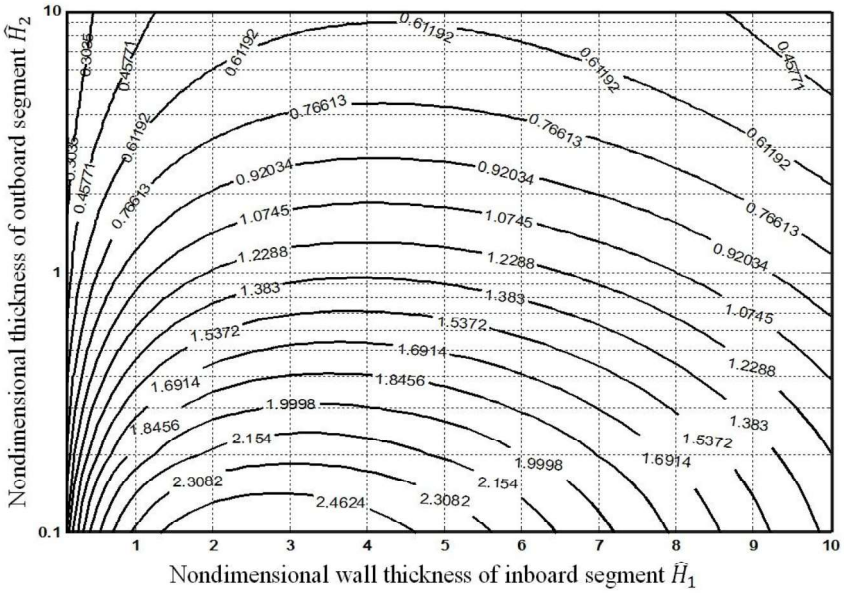

Figure 7 Effect of wall thickness on nondimensional bending frequency of a two-segment spar

The effect of segment length and wall thickness on the second bending or extension-dominated frequency is shown in Fig. 8. It is observed that the whole domain is divided into two distinct regions in which the upper one contains the global minimum while the lower one contains two local maxima at $\hat{L}_2$=0.25 and $\hat{L}_2$=0.75. This result indicates the importance of studying the higher modes of vibrations in the case of multiple-segment blade optimization. Thus, maximization of the fundamental frequencies alone doesn't guarantee maximization of other higher frequencies.

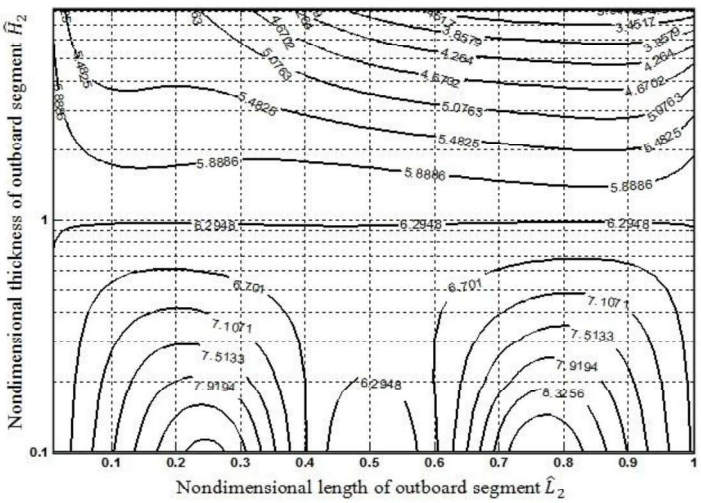

Figure 8 Effect of length and thickness of the outboard segment on nondimensional bending or extension-dominated second mode frequency of a two-segment spar

5. Conclusions

An efficient analytical model is developed for studying the coupled vibration of a wind turbine blade spar. Based on the fact that an exact dynamic analysis of uniform thin-walled beam segment is available and well established, the dynamic analysis of tapered blade spar has been obtained by applying the transfer matrix method. The main conclusions that can be revealed from the present work are:

1- Tapered multiple-segment spar with spanwise material grading gives natural frequencies higher than that of the reference design. However, it is proved that maximization of the fundamental frequency alone doesn't guarantee maximization of the other higher frequencies. Higher frequencies have been found to have many local minima and maxima in the defined design space
2- There are optimum design variables of each segment such as the length, height, wall thickness and fiber content at which the structural dynamic performance can be enhanced. Good designs favor minimum wall thickness and higher fiber volume fraction.

Finally, the analytical model formulated in the present study can be extended and applied to study the forced dynamic response of a wind turbine blade. Other cross sectional types of the blade spar, such as D-shape spar, can be considered and the effects of blade twist, shear deformation, and rotary inertia are under investigation by the authors.

References

[1] R. Gasch, J. Twele, Wind Power Plants, New York, Springer, 2012.
[2] Ibrahim Al-Bahadly**,** Wind Turbines, InTech, ISBN: 978-953-307-221-0, 2011, http://www.intechopen.com/books/wind-turbines.
[3] E. A. Armanios and A. M. Badir, Free vibration analysis of anisotropic thin-walled closed-sections beams**.** AIAA, Vol. 33, No.10, 1995, 1905-1910.
[4] D.S. Dancila and E.A. Armanios, The influence of coupling on the free vibration of anisotropic thin-walled closed-section beams, Int. J. Solids Structures, Vol. 35, No.23, 1998, 3105-3119.
[5] K.Y. Maalawi, Dynamic optimization of functionally graded thin-walled box beams, International Journal of Structural Stability and Dynamics, Vol.17, No.9, 2017, 1750109-1, 24.
[6] I.M. Daniel and O.Ishai, Engineering Mechanics of Composite Materials, 2nd edition, NewYork, Oxford, University Press, 2006.
[7] T. Alexander, F. Ludovit, Transfer Matrix Method, Kluwer Academic Publisher, 1988.
[8] G.S. Bir, F. Oyague, Estimation of Blade and Tower Properties for the Gearbox Research Collaborative, National Renewable Energy Laboratory, U.S. Department of Energy, 2007.
[9] D. Gay, S.V. Hoa, Composite Materials: Design and Applications, New York, CRC Press, 2007.